PERGAMON

Mechatronics 12 (2002) 1097–1114

MECHATRONICS

A smart boring tool for process control

Byung-Kwon Min *, George O'Neal, Yoram Koren, Zbigniew Pasek

Department of Mechanical Engineering, The University of Michigan, 2250 Hayward Ave., Ann Arbor, MI 48109-2125 USA

Abstract

A mechatronic metal cutting tool has been developed to improve the accuracy and flexibility of line boring machining in the automotive industry. Laser position sensors and piezoelectric actuator were integrated into the rotating body of the boring tool. To compensate the boring bar droop and effects of cutting forces, a fast tool servo utilizing feedback control of the boring tool insert position was designed and embedded in the rotating tool assembly. In addition to position control, a self-monitoring algorithm that utilizes disturbance estimator has been put together in the controller. Experimental results demonstrated that the developed cutting process controller improves the accuracy of the boring tool as well as reliably detects the process failures, such as tool tip breakage, without additional monitoring equipment.

Keywords: Tool servo; Machine tool; Condition monitoring; Piezoelectric

1. Introduction

Recent changes in the automotive market are driving a need for new engine manufacturing technologies that provide flexibility at an affordable cost. Although the introduction of CNC machines into automotive engine production systems increased the level of flexibility, the need for specialized boring tools for cam and crankshaft holes (referred to as line boring tools) remains one of the major difficulties in introducing CNC machine tool with tool changers. Fig. 1(a) shows the

* Corresponding author. Tel.: +1-734-764-5528; fax: +1-734-615-0312.
E-mail address: bkmin@umich.edu (B.-K. Min).

0957-4158/02/$ - see front matter © 2002 Published by Elsevier Science Ltd.
PII: S0957-4158(02)00020-X

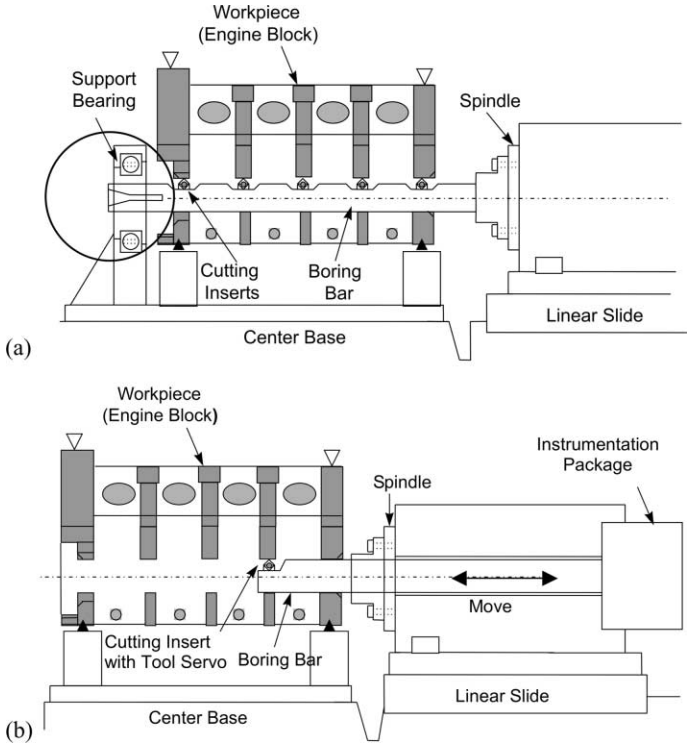

Fig. 1. Structure of line boring machines: (a) conventional line boring tool with outboard support and multiple cutting inserts, (b) concept design of Smart Tool line boring system.

traditional line boring process. To avoid tool droop the boring bar is typically supported on both ends. This outboard support bearing required in traditional boring is one of the major obstacles to automated tool changes.

A new type of boring tool called *Smart Tool* has been developed to increase agility and flexibility at the boring station. The concept of the Smart Tool line boring system layout is presented in Fig. 1(b). This new design allows the boring bar to be used with an automated tool changer and a standard tool interface by the elimination of support bushings. An on-line compensation mechanism relying on an active tool-tip servo with a piezoelectric actuator is used to compensate for the increased compliance of the unsupported long boring bar. The Smart Tool also includes an internal cutting force measurement method utilized for process monitoring. This monitoring function improves the Smart Tool reliability and reduces the need for external monitoring equipment.

In Section 2 the critical issues in the line boring process are explained. The structure of the Smart Tool is presented in Section 3 as an improvement to traditional boring tools. In Section 4 the Smart Tool servo system is modeled. Then design and experimental verification of the tool tip position controller including an

on-tool cutting force estimator is discussed. Section 5 focuses on the monitoring method for process monitoring utilizing the controller.

2. State of the art

Line boring tools described in this paper are characterized by high length-to-diameter (L/D) ratios. They are typically fixed to a rotating spindle at one end, with a cutting insert attached to the free end, though multiple supports and inserts are often used. Boring bars with large L/D ratios typically have low dynamic stiffness making them susceptible to mechanical vibrations that result in poor part quality and short tool life. Substantial amount of research and many practical applications have focused on methods to limit unwanted vibration in cutting operations, allowing for boring with large L/D ratios.

Much of the research in the boring area has focused on vibration reduction related to either one of two sources: forced vibration (due to cutting forces and mass unbalance) or self-excited vibration (chatter). Studies to eliminate or reduce vibration explore either passive or active methods. Passive methods include use of materials with high elastic modulus and use of passive dynamic vibration absorbers [1,2]. Kim et al. [3] used forecasting compensatory control to construct an auto regressive stochastic model of the cylindricity error by laser measurement. Based on the forecasted error signals, a feed forward controller generated a control command to compensate. Active vibration absorbers [4] and active chatter control at the boring tool clamp [5] have been used in machining to improve the vibration characteristics of the tool. Hanson and Tsao [6] developed a variable-depth-of-cut machining approach which uses a fast tool servo to eliminate the error between the desired and actual tool positions by feed-forward or repetitive control. It has to be stressed, however, that most of the reviewed works focused on standard boring processes without utilizing a tool servo, or addressed similar applications such as turning.

Process monitoring has an important role in automated manufacturing plants. Rapid detection and isolation of failures and their root causes increases process reliability and productivity, and reduces downtime. In machining processes, tool breakage and faulty tool condition are critical failures affecting part quality and production cost, and, therefore, have been intensively investigated during the past three decades [7,8].

Various direct and indirect monitoring devices, including acoustic sensors, tool dynamometers, force sensors, and machine tool motor current sensors have been used for tool condition monitoring purposes. Even though the use of tool dynamometer has been a frequently accepted method of tool condition monitoring in research environments, adding a tool dynamometer to a machine tool is not always feasible due to the difficulties in the integration and its effects on the machine tool dynamics. In addition, the high cost of the tool dynamometer makes its use uneconomical in industrial applications. Recently introduced commercial tool condition monitoring systems using load cells are more affordable than the tool dynamometer [9].

3. Structure of Smart Tool

The proposed Smart Tool adopted a fast tool servo that utilizes a piezoelectric actuator and two laser photo sensors to actively isolate the cutting insert from erroneous bar motions while rejecting cutting force disturbances.

The purpose of the tool tip servo is to isolate the cutting insert from erroneous boring bar motions (i.e., deviations from a perfectly cylindrical path) while rejecting cutting force disturbance. This servo has to be fast enough to compensate for at least the forced vibration due to spindle rotation at 6000 rpm. The layout of the Smart Tool system is presented in Fig. 2. The tool body contains a position sensor and the actuation mechanism. The instrumentation package including an embedded computer controller is located in a cylindrical container attached to the back of machine spindle and rotates with the spindle.

The proposed Smart Tool consists of: (i) measurement system, (ii) computer controller, (iii) cutting insert, (iv) tool tip translation mechanism, (v) piezoelectric actuator, and (vi) power and data transmitter.

Two position-sensitive optical detectors, measuring the position of the cutting insert and the deflection of the boring bar relative to the spindle, provide the real-time feedback signals. The detector measuring the position of the cutting tool is a single axis bi-cell detector. The detector measuring the deflection of the boring bar is a two-dimensional continuous position sensitive detector. The single-axis and two-dimensional sensors used in the method have a resolution of about 0.3 and 1 μm respectively. The use of position sensitive optical detectors is based on the assumption that the motion error of the precision spindle around its center is negligible or deterministic.

Two laser beams are produced by splitting the beam from a semiconductor laser using a beam splitter. The laser and the focusing optics are located on the axis of rotation. One beam passes through the axis to the detector attached to the cutting tool. The second beam is directed to an off-axis detector attached to the end of the boring bar.

The controller is implemented with a microcomputer (PC/104 computer with 133 MHz AMD 5 X 86 CPU, 16-bit off-the-shelf analog to digital converters, and a 16-bit digital to analog converter) in the instrumentation package shown in the figure. All control algorithms are embedded in the controller using an on-board flash memory. The control loop has a 150 μs sampling period. The Smart Tool controller communicates with the machine controller using a standard serial data port. The machine controller can start and stop the control loop, and upload and download data and parameters to and from the Smart Tool.

The tool tip translation mechanism enables actuation of the cutting insert in the depth of cut direction exclusively. In the ideal case, the translation mechanism should constrain the cutting insert to rectilinear motion. The translation mechanism also provides the preload to the piezoelectric actuator, thus the connection to the piezoelectric actuator only needs to transfer compressive loads, allowing it to be a simple point contact. The mechanism is dynamically balanced to reduce rotational effects. The cutting insert is attached to the flexure mechanism, enabling its motion relative to the tool body.

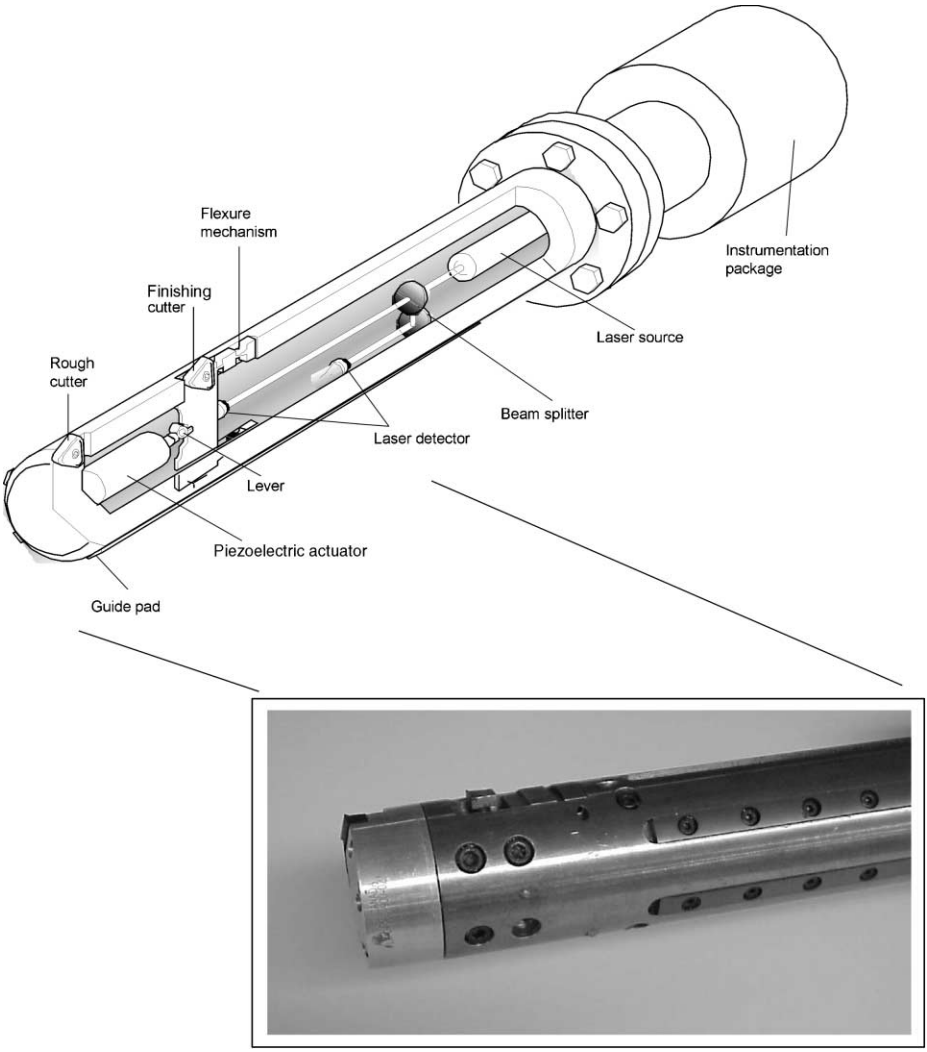

Fig. 2. Smart Tool.

A piezoelectric stacked actuator provides the actuation force to the flexure mechanism. A piezoelectric actuator is used for its large power to volume ratio and high operating frequency. A lever connecting the actuator with the tool tip translator enables magnification of its displacement. Rated electrical power necessary to run the piezoelectric actuator is 150 V and 2 A.

To supply power to the piezoelectric actuator and controller computer that are rotating with the boring tool, a non-contact power/data transformer is employed. The disk type inductive power/data transformer located at the end of rotating

instrumentation package allows transmission of 500 W of power at peak is transmitted. The non-contact power/data transformer also transfers the data from serial communication port using modulated duplex data signal with speed up to 20 kbps.

4. Tool tip servo control and force measurement of Smart Tool

4.1. Smart Tool model

Piezoelectric material has the property of changing shape in an electric field, allowing it to be used as an electromechanical transducer. A piezoelectric actuator behaves like a spring with a variable free length and distributed mass as depicted in Fig. 3. The free length of the spring in the model is approximately proportional to

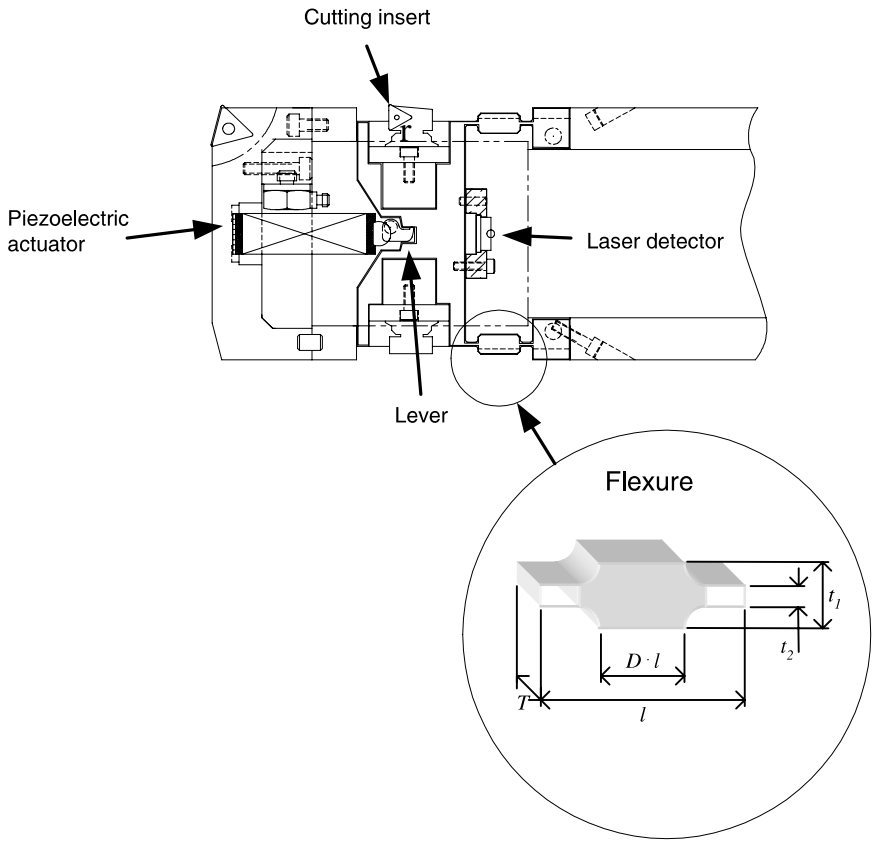

Fig. 3. Detail of Smart Tool servo mechanism.

the applied voltage. The compression force in the piezoelectric actuator can be approximated by the following formula.

$$F_{\mathrm{p}} = K_{\mathrm{p}} + f_{\mathrm{a}} = -\frac{A_{\mathrm{p}} Y_{33}^{E}}{l_{\mathrm{p}}} \Delta x + A_{\mathrm{p}} \frac{Y_{33}^{E} d_{33}}{H} V, \tag{1}$$

where A_{p}, l_{p}, H, Y_{33}^{E}, d_{33} and Δx are the area, length, layer thickness, Young's Modulus, strain constant and extension of the piezoelectric actuator, respectively.

It is assumed that the piezoelectric actuator has negligible mass, hysteresis and drift. The second term, f_{a}, represents the control force, which is controlled by voltage supplied from the power amplifier. Both terms of Eq. (1), the first term, K_{p}, the stiffness of the piezoelectric actuator, and the second term, f_{a}, are subject to saturation in both amplitude and time rate of change. These non-linearities are characteristics of the piezoelectric material and power amplifier properties. Since piezoelectric material begins to depolarize under the influence of strong electric fields, manufacturers specify a maximum allowable electric field.

Details of Smart Tool servo mechanism is depicted in Fig. 3. The proposed design of the tool tip servo mechanism is based on flexure structure. From solid mechanics principles, the stiffness to an actuating force, K_l, is estimated by equation,

$$K_l = 2\frac{E_t T}{l^3}\left(\left(\frac{1}{t_2^3} - \frac{1}{t_1^3}\right) D^3 + \frac{1}{t_1^3}\right)^{-1}, \tag{2}$$

where E_t, T, l and t_1 are the elastic modulus, width, length and thickness of the flexure.

The flexure has an increased cross-sectional area in its middle section to increase the ratio of the compliance in the drive direction to that in the perpendicular direction. Dl is the length and t_2 is the thickness of this center section.

To model the boring bar, a first mode approximation of a boring bar is obtained by assuming the bar to be a fixed-free cantilever beam. The natural frequency (ω_{n}), equivalent stiffness (K_{b}) and equivalent mass (M_{b}) of the first mode of a cantilever beam are approximated by

$$\omega_{\mathrm{n}} = 3.52\sqrt{\frac{E_{\mathrm{b}} I}{m_{\mathrm{b}} l_{\mathrm{b}}^4}} \tag{3}$$

$$K_{\mathrm{b}} = 3\frac{E_{\mathrm{b}} I}{l_{\mathrm{b}}^3} \tag{4}$$

and

$$M_{\mathrm{b}} = \frac{K_{\mathrm{b}}}{\omega_{\mathrm{n}}^2}, \tag{5}$$

where m_b, l_b, E_b, and I are the mass per unit length, length, elastic modulus and area moment of inertia, respectively, of the boring bar.

4.2. Tool tip servo controller design

The purpose of tool tip controller is to isolate the tool tip from any erroneous non-cylindrical motion of the boring bar, holding the tool tip still relative to the spindle in the face of disturbances. A laser system described in Section 3 is being designed to provide the controller with the displacement of the tool tip and boring bar relative to the spindle center. A digital feedback controller has been designed to implement in the controller computer inside Smart Tool.

Using the system parameters derived in the previous section, the Smart Tool system, including flexure mechanism and boring bar, can be modeled as an equivalent mass–spring–damper model as depicted in Fig. 4. The model of the Smart Tool system is given by

$$\begin{aligned}
\frac{\partial}{\partial t}\begin{bmatrix} x_b \\ \dot{x}_b \\ \Delta x \\ \Delta \dot{x} \end{bmatrix} &= \begin{bmatrix} 0 & 1 & 0 & 0 \\ -\dfrac{k_b}{M_b} & -\dfrac{b_b}{M_b} & \dfrac{K_p + K_I}{M_b} & \dfrac{b_m}{M_b} \\ 0 & 0 & 0 & 1 \\ \dfrac{k_b}{M_b} & \dfrac{b_b}{M_b} & -(K_p + K_I)\left(\dfrac{1}{M_b} + \dfrac{1}{M_m}\right) & -b_m\left(\dfrac{1}{M_b} + \dfrac{1}{M_m}\right) \end{bmatrix} \begin{bmatrix} x_b \\ \dot{x}_b \\ \Delta x \\ \Delta \dot{x} \end{bmatrix} \\
&\quad + \begin{bmatrix} 0 \\ \dfrac{1}{M_b} \\ 0 \\ -\left(\dfrac{1}{M_b} + \dfrac{1}{M_m}\right) \end{bmatrix} f_a + \begin{bmatrix} 0 \\ 0 \\ 0 \\ -\dfrac{1}{M_m} \end{bmatrix} w, \\
y &= \begin{bmatrix} 1 & 0 & 1 & 0 \end{bmatrix} \begin{bmatrix} x_b \\ \dot{x}_b \\ \Delta x \\ \Delta \dot{x} \end{bmatrix},
\end{aligned} \tag{6}$$

where $\Delta x = x_m - x_b$, y is the estimated tool tip position, w is the cutting force input into the Smart Tool, and M_m is the mass of the tool tip servo mechanism.

Since digital controller with 150 μs sampling period is used for Smart Tool, including the zero-order-holder on the input, the system is converted to standard notation in discrete form. Eq. (6) becomes

$$\begin{aligned}
\mathbf{x}(k+1) &= \mathbf{A}\mathbf{x}(k) + \mathbf{B}u(k) + \mathbf{N}w(k), \\
y(k) &= \mathbf{C}\mathbf{x}(k),
\end{aligned} \tag{7}$$

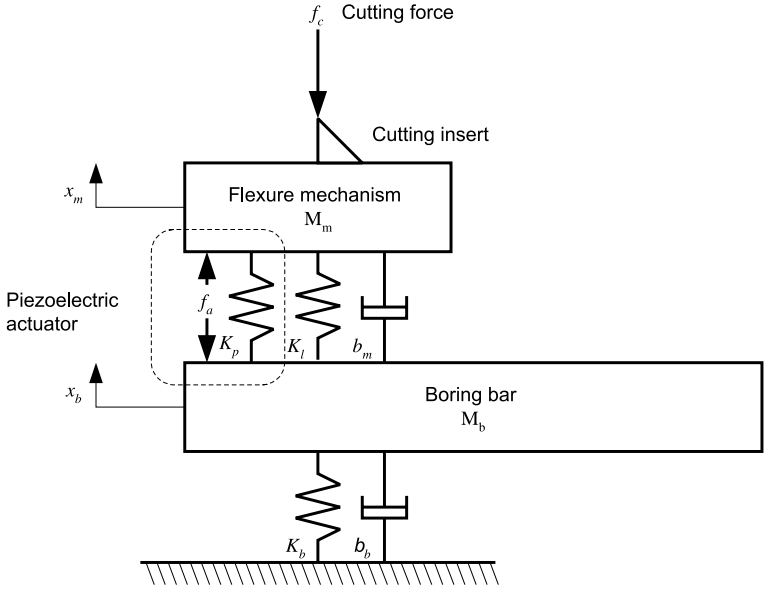

Fig. 4. Mass–spring–damper model of Smart Tool.

$$\text{where } \mathbf{A} = \begin{bmatrix} 0.7651 & 0.1355 & 0.2343 & 0.0145 \\ -2.9610 & 0.7336 & 2.9454 & 0.2653 \\ 0.0348 & 0.0022 & 0.9532 & 0.1469 \\ 0.4376 & 0.0395 & -0.5956 & 0.9446 \end{bmatrix}, \quad \mathbf{B} = \begin{bmatrix} -1.2335 \\ -15.5451 \\ 0.1829 \\ 2.2977 \end{bmatrix},$$

$$\mathbf{N} = \begin{bmatrix} -0.0003 \\ -0.0064 \\ -0.0049 \\ -0.0647 \end{bmatrix}, \quad \text{and} \quad \mathbf{C} = [1 \quad 0 \quad 1 \quad 0].$$

The values for **A**, **B**, **C**, and **N** were determined based on the design parameters of the Smart Tool described in Table 1 and then refined by system identification experiment which applied static cutting force to the Smart Tool.

The feedback controller has been designed in the form of Eq. (8)

$$u(n) = -\mathbf{K}\mathbf{x}(n). \tag{8}$$

The gain vector **K** is chosen to minimize the quadratic cost function J in Eq. (9).

$$J = \sum_{n=0}^{\infty} \mathbf{x}^{\mathrm{T}}(n) \cdot \mathbf{Q} \cdot \mathbf{x}(n) + u^{\mathrm{T}}(n) \cdot \mathbf{R} \cdot u(n). \tag{9}$$

The parameter J is a weighted sum of the states and the control inputs. The weighting factors **Q** and **R** were tuned first based on simulations and then refined by experiments.

Table 1
Model parameters

Variable	Value
Piezoelectric actuator	
Young's modulus Y_{33}^E (Pa)	4.8×10^{10}
Strain constant d_{33} (m/V)	5.5×10^{-8}
Max. voltage V_{max} (V)	100
Density m_p (kg/m^3)	7500
Max. current I_{max} (A)	2.0
Area A_p (m^2)	1.0×10^{-4}
Length l_p (m)	0.04
Tool tip translation mechanism	
Width T (m)	0.025
Mass M_m (kg)	0.15
Length l (m)	0.016
Damping b_m (N s/m)	0.025
Length Dl (m)	0.01
Young's modulus E_t (Pa)	2×10^{11}
Boring bar	
Moment of inertia I (m^2 kg)	7.1×10^{-7}
Young's modulus E_b (Pa)	2×10^{11}
Ultimate strength S_{ut} (N)	1.4×10^{11}
Damping b_b (N s/m)	0.013
Yield strength S_e (N)	3.4×10^{10}

The proposed full-state feedback control scheme requires knowledge of all the states of the control system. However, since the Smart Tool uses sensors to measure only tool tip and bar end positions, an observer must be used to estimate the remaining states.

Furthermore, cutting force needs to be measured and compensated to improve the performance of the tool tip servo. Measuring the radial cutting force on a conventional machine tool requires special equipment, such as a tool dynamometer or spindle torque monitor. However, by implementing a disturbance estimator in the tool tip servo controller, the Smart Tool can estimate cutting force. In this system the external disturbance to the servo is exactly the same as cutting force. For this purpose, an observer model implemented in the Smart Tool includes cutting force dynamics as well as the dynamics of the Smart Tool. This estimated cutting force is then utilized for controlling the position of the tool tip and subsequently used for the process monitoring that will be discussed in the next section. As a result of the tool servo flexure mechanism design, deployed between the cutter and tool actuator, only the radial direction component of the cutting force acts as a disturbance to the tool servo. Therefore, throughout this paper only the radial cutting force is referred to as a cutting force.

The Smart Tool system equation modeled by the Eq. (7) is expanded with cutting force disturbance as internalized states of the system. A discrete state space model of the cutting force disturbance is generated by assuming that the disturbance has the following structure as suggested in [10].

$$\begin{aligned}\mathbf{x}_{\mathrm{d}}(k+1) &= \mathbf{\Phi}_{\mathrm{d}}\mathbf{x}_{\mathrm{d}}(k),\\ \mathbf{w}(k+1) &= \mathbf{H}_{\mathrm{d}}\mathbf{x}_{\mathrm{d}}(k),\end{aligned} \tag{10}$$

where $\mathbf{x}_{\mathrm{d}}$ is a state vector of the cutting force that is same as disturbance to the Smart Tool, $\mathbf{w}(k)$ is the estimate of the cutting force, and the matrix $\mathbf{H}_{\mathrm{d}}$ is relation between $\mathbf{x}_{\mathrm{d}}$ and $\mathbf{w}(k)$.

The matrix $\mathbf{\Phi}_{\mathrm{d}}$ in Eq. (10) describing disturbance dynamics depends on what is perceived to be the dominant dynamic component of the cutting force. The cutting force in Smart Tool controller is dominated by a sinusoidal and a constant component, due to the rotation of the spindle during the boring process.

The sinusoidal component of the cutting force (which has an impulse response that is a sinusoid) as well as the constant component of the cutting force can be modeled using the state space model in Eq. (11).

$$\begin{bmatrix} x_{\mathrm{d}1}(k+1)\\ x_{\mathrm{d}2}(k+1)\\ x_{\mathrm{d}3}(k+1)\end{bmatrix} = \begin{bmatrix} 0 & 1 & 0\\ -1 & 2\cos(T_{\mathrm{s}}\omega_0) & 0\\ 0 & 0 & 1\end{bmatrix}\begin{bmatrix} x_{\mathrm{d}1}(k)\\ x_{\mathrm{d}2}(k)\\ x_{\mathrm{d}3}(k)\end{bmatrix}. \tag{11}$$

The system in Eq. (11) has a sinusoidal response with a tooth frequency of ω_0 which equals to the frequency of the spindle rotation because Smart Tool has only one tooth. The parameter T_{s} is the sampling time of the controller.

Therefore, $\mathbf{\Phi}_{\mathrm{d}}$ and $\mathbf{H}_{\mathrm{d}}$ in Eq. (10) to model the cutting force with the sinusoidal and constant components have the following form.

$$\mathbf{\Phi}_{\mathrm{d}} = \begin{bmatrix} 0 & 1 & 0\\ -1 & 2\cos(T_{\mathrm{s}}\omega_0) & 0\\ 0 & 0 & 1\end{bmatrix}, \tag{12}$$

and

$$\mathbf{H}_{\mathrm{d}} = [\,0 \quad 1 \quad 1\,]. \tag{13}$$

The Smart Tool dynamics augmented with the cutting force states are given in Eq. (14). In this augmented form, the input to the system is the voltage applied to piezoelectric actuator and the output of this model, $y(k)$, is the tool tip position. The cutting force state is internalized.

$$\begin{aligned}\begin{bmatrix}\mathbf{x}(k+1)\\ \mathbf{x}_{\mathrm{d}}(k+1)\end{bmatrix} &= \begin{bmatrix}\mathbf{A} & \mathbf{N}\mathbf{H}_{\mathrm{d}}\\ \mathbf{0} & \mathbf{\Phi}\end{bmatrix}\begin{bmatrix}\mathbf{x}(k)\\ \mathbf{x}_{\mathrm{d}}(k)\end{bmatrix} + \begin{bmatrix}\mathbf{B}\\ \mathbf{0}\end{bmatrix}u(k),\\ y(k) &= [\,\mathbf{C} \quad \mathbf{0}\,]\begin{bmatrix}\mathbf{x}(k)\\ \mathbf{x}_{\mathrm{d}}(k)\end{bmatrix}.\end{aligned} \tag{14}$$

Since $\mathbf{x}$ and $\mathbf{x}_{\mathrm{d}}$ are observable, a Kalman filter [11] is used to design an estimator for these states in real time. Plant disturbances and measurement noise in the form of white noise with a Gaussian distribution are assumed to be the source of observation errors in the Kalman filter. The controller can be properly tuned to achieve a compromise between faster estimator dynamics and filtering of the laser position sensor signal.

This controller was designed to reject cutting forces, while tracking references to tool tip position. With the **Q** and **R** for Eq. (9) selected as

$$\mathbf{Q} = \begin{bmatrix} 10 & 0 & 0 & 0 \\ 0 & 10 & 0 & 0 \\ 0 & 0 & 1 & 0 \\ 0 & 0 & 0 & 1 \end{bmatrix}$$

and $\mathbf{R} = 2000$, the feedback gain **K** is given in Eq. (15).

$$\mathbf{K} = [0.0745 \quad -0.0361 \quad -0.0874 \quad -0.0087]. \tag{15}$$

The block diagram of the overall structure final design of the controller and monitoring system is shown in Fig. 5. The cutting force estimated in real-time is used for both disturbance rejection in control and monitoring of the Smart Tool. Since the reference input of the system is desired tool tip position, the feed forward term in the figure, K_f, should be obtained from the relation between plant input and output as described in [10]. The monitoring algorithm analyzes the force signal based on the method described in the next section in order to identify the failure of the cutting process.

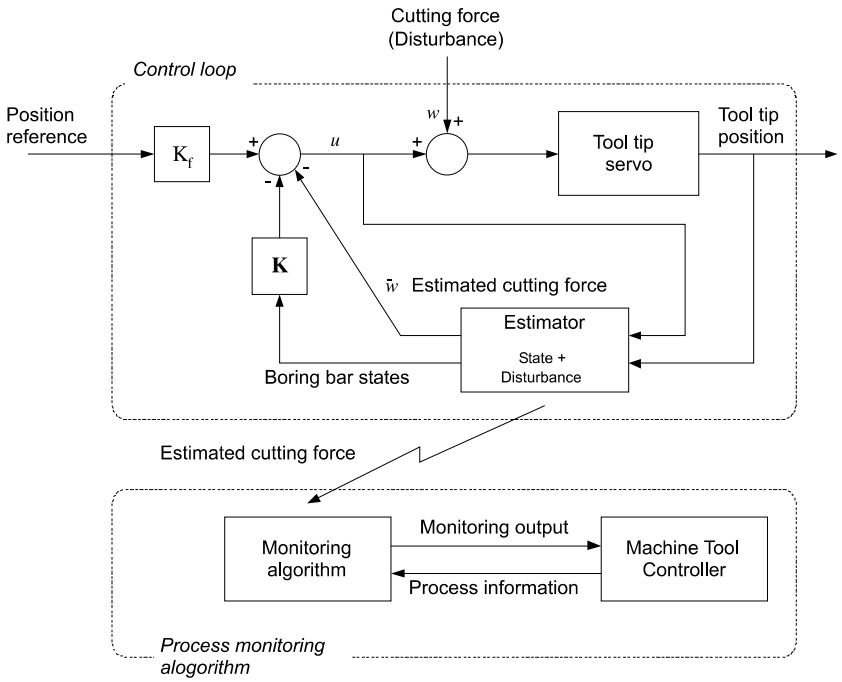

Fig. 5. Block diagram of Smart Tool control and monitoring.

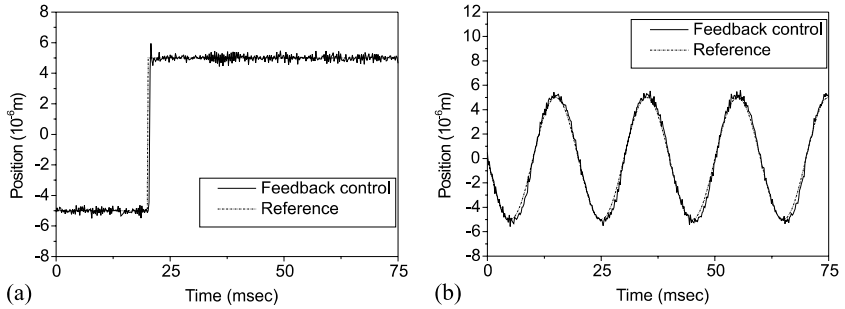

Fig. 6. Position control results: (a) step response (feedrate 0.21 mm/rev; cutting speed 4.8 m/s), (b) sinusoidal response (feedrate 0.21 mm/rev; cutting speed 4.8 m/s).

4.3. Experimental result of tool tip servo control

In order to evaluate the performance of the tool tip servo under real machine tool operating conditions, cutting tests were performed using a stationary Smart Tool boring bar and rotating workpiece. For the cutting test, an aluminum workpiece made from thick wall tube with a 180 mm diameter hole was used. The Smart Tool boring bar was attached to a turning machine tool post and the workpiece was attached to spindle. The tool tip position measurement was recorded to the memory of the controller computer. The spindle speed was 510 rpm corresponding to a cutting speed of 4.8 m/s. The feedrate was 0.21 mm/rev. Step response and sine wave tracking were conducted. The purpose of the step response experiment was to determine what tolerances could be maintained in the position of the tool tip relative to the fixture, as well as the effects of cutting on the transient response of the tool tip servo. The purpose of the sine wave tracking experiment was to verify the ability of the system to follow sinusoidal references during cutting. This is similar to the objective of isolating the tool tip motion from boring bar vibration.

As can be seen in Fig. 6(a), the tool tip servo responded to step references of 10 μm. The controller maintained the tool tip position relative to the fixture to within 1 μm during the cutting operation and the rise time was less than a 0.001 s. Another experimental result for sine wave tracking are shown in Fig. 6(b). Similarly to the step response result, the error using the closed loop controller could be maintained within 1 μm.

5. Monitoring of cutting process

Cutting force estimation derived by the method proposed in Section 4 is applied to boring process monitoring. The typical process failures of the line boring process are geometric error related to workpiece fixture misalignment and cutting tool insert breakage.

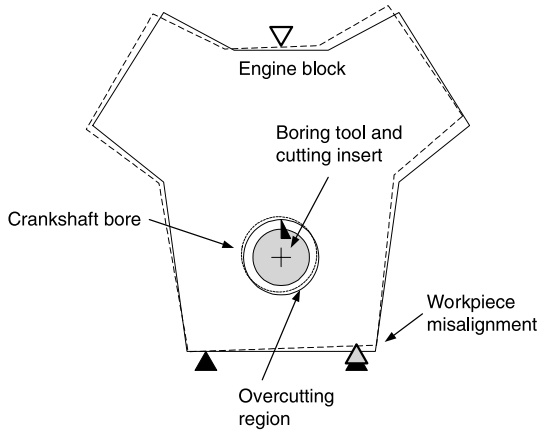

Fig. 7. Non-uniform depth of cut due to workpiece misalignment error.

Fig. 7 illustrates the geometry of finish boring process. As can be seen, if the center of the pre-boring hole and the finish boring tool position are offset due to fixture misalignments, the depth of cut of the boring process becomes a periodic function that is repeated with every revolution of the spindle. Tool breakage also results in the deviation of the cutting force from the normal cutting force generated by the boring process. Cutting force is a monotonic function of the depth of cut and feed [8]. Consequently, if the feed is maintained constantly and if the cutting force is accurately measured, the geometric profile of the cutting surface can be estimated from the force data.

Cutting tool insert breakage can be monitored in a cutting force changes. For a boring process, the radial direction component of the cutting force dramatically increases immediately after tool fracture or chipping [12]. Considering the small cutting force generated by finishing process, an excessive rise in the radial cutting force generally indicates finish tool breakage, if the force is bigger than that observed in workpiece misalignment error which will be detailed in the rest of this section.

Based on above observation, the monitoring of fixture misalignment and tool breakage of the Smart Tool boring process can be carried out with force pattern recognition. The radial cutting force estimation described in the previous section has been considered as a method for the monitoring of the Smart Tool boring process. The cutting force estimated by Smart Tool during a single rotation is compared with the radial cutting force measured by a tool dynamometer in a polar plot in Fig. 8(a). Cutting speed was 2.0 m/s and feedrate was 0.083 mm per revolution. A random cutting profile was used to evaluate dynamic performance of the estimator. The difference between the Smart Tool estimation and the tool dynamometer measurement was less than 10% of the cutting force and, thus, the cutting force based on disturbance estimation could be used to detect both the dynamic and the static cutting forces.

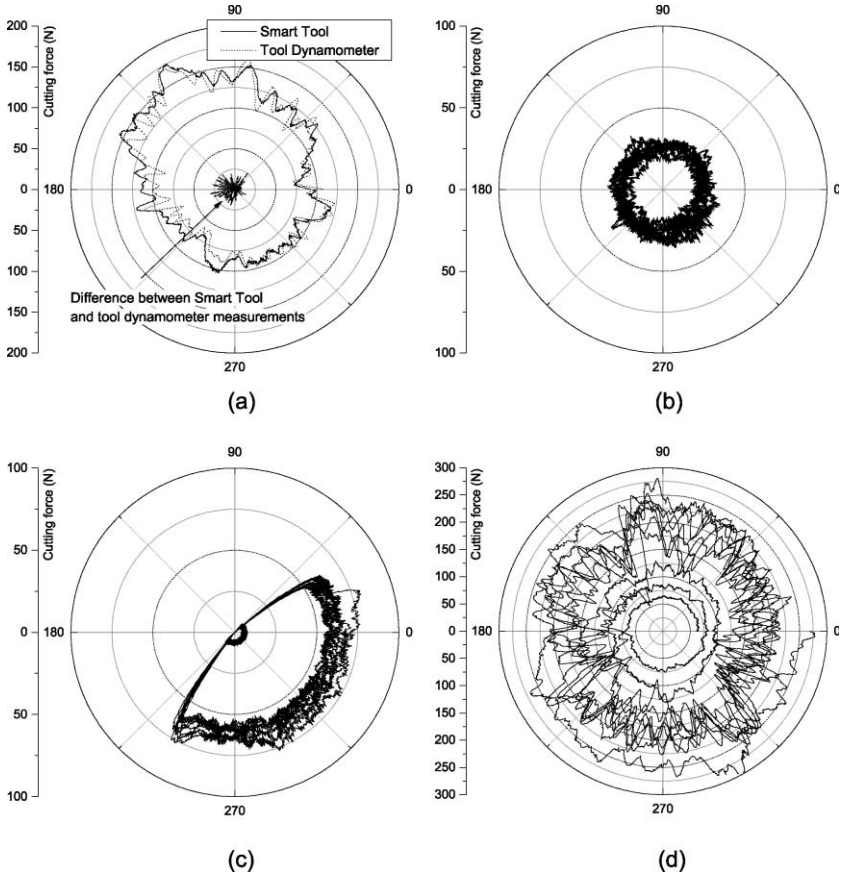

Fig. 8. Cutting force measured at Smart Tool. Depth of cut 0.25 mm; feedrate 0.083 mm/rev; cutting speed 2 m/s. (a) Comparison with tool dynamometer measurement, (b) normal cutting, (c) workpiece misaligned (tool offset 1.27 mm), (d) tool breakage.

Fig. 8(b) shows the polar plot of cutting force during a normal boring process operation. Fig. 8(c) and (d) show the case of workpiece misalignment error and the event of tool breakage respectively. Cutting condition of 2 m/s cutting speed and 0.083 mm per revolution federate was used for all experimental data. 0.25 mm depth of cut is used for normal cutting and 0.25 mm desired depth of cut with 1.27 mm offset was used for misalignment experiment. For the tool breakage experiments, inserts with a 2.0 mm notch was used to expedite breakage.

For the normal operation, as can been in Fig. 8(b), the cutting force has not deviated more than 10 N from its mean value of 25.96 N and the center of the force plot is close to the center of the graph. The response from misaligned cutting plotted in Fig. 8(c) also shows regular cutting force, but the center of the force plot is shifted from the graph center. The small partial circle in the plot is due to the negative reaction force of the tool when the cutting insert lost the contact with workpiece.

The tool breakage recorded in Fig. 8(d) shows the chaotic behavior of the cutting force with huge force value.

As can be seen the plots in Fig. 8, it is obvious that the different process failures have different force patterns. Therefore, if the difference between the force patterns can be specified quantitatively, monitoring of these failures is available.

Least squares center and *circle* are introduced for quantitative analysis of force pattern. The least square circle center is a center which minimizes the sum of the squares of the polar plot deviations from a circle about the center. Approximate formulae [13] are used for real-time calculation. Using the approximate method, the distance between least square center and original coordinate center, that is same as the tool center, r, is calculated as described in Eq. (16).

$$\begin{aligned} a &= \frac{2 \times \text{sum of } x \text{ values}}{\text{number of ordinates}} = \frac{2\sum x_i}{n}, \\ b &= \frac{2\sum y_i}{n}, \text{ and} \\ r &= \sqrt{a^2 + b^2}. \end{aligned} \tag{16}$$

The radius of the least square circle, R is

$$R = \frac{\text{sum of radial values}}{\text{number of ordinates}} = \frac{\sum f_i}{n}. \tag{17}$$

In this experiment, the R and r values calculated from 10 most recent revolutions are used. The R is equal to mean value cutting force. Therefore, regardless of existence of workpiece misalignment error, the excessive R value bigger than critical value is due to tool breakage. The critical cutting force of the tool breakage must be determined by experiment. In this experiment, it is set to 129.80 N which is 500% of measured cutting force, 25.96 N, from normal operation plotted in Fig. 8(b).

As far as the mean cutting force R is smaller than critical value, the bigger r value indicates workpiece misalignment error. The threshold of r value is also determined by experiment. In the experiment, it is set to 5.19 N which is 20% of normal operation cutting force. This also means threshold of the offset is approximately 20% depth of cut, even though that is not exact number due to non-linear relation between cutting force and depth of cut. From a and b values, which are x- and y-directional components of the radial cutting force, the misalignment direction of the hole can be found. The a, b, R, r, and direction of least square center,

Table 2
Monitoring variables

Process status	a	b	R (129.80)	r (5.19)	θ
Normal	1.08	0.50	25.96	1.19	24.95
Workpiece misalignment	30.79	−29.17	24.79	42.58	−43.44
Tool breakage	5.09	3.34	150.93	6.78	29.48

The values in parantheses indicate critical values.

θ are arranged in Table 2. As can be seen in the table, R and r are effective in monitoring.

6. Conclusion

The paper focused on an effort to develop a smart boring tool supporting agility and flexibility at the station level by providing feedback control embedded in the tool. Self-monitoring capability is an important feature in automated machine tool systems and it is more critical when sophisticated mechatronics is used to control the process. This paper has proposed a tool monitoring method that utilizes the process information and estimated cutting force during tool tip servo control. A new measurement technique of the cutting force based on disturbance estimation was developed and integrated into a sensorized boring tool.

Through experiments highlighted in the paper, it was demonstrated that the proposed tool tip servo controller can successfully operate with position error smaller than 1 μm during cutting. The proposed cutting process monitoring method was effective to detect tool failure as well as process failure due to workpiece misalignment errors which occurred in the boring process.

The force measurement by the proposed method matches well with the conventional force measurement using a tool dynamometer. The developed accurate cutting force estimation method is not only useful for process failure monitoring, but it is also useful as a substitute for tool dynamometers, especially in cases where the tool dynamometer is difficult to be placed, such as in a rotating tool tip.

The paper demonstrated the benefit of introducing mechatronic approach into the traditional tooling of manufacturing machinery. The electronic package and the new algorithm embedded in the Smart Tool made it possible to build a self-contained tool-tip position controller with self-monitoring inside a rotating cutting tool, thus increasing the productivity and the reliability of the boring process.

Acknowledgements

The research was sponsored in part by the NSF Engineering Research Center for Reconfigurable Machining System under NSF grant # EEC-9529125 and in part by NIST ATP grant # 70NANB5H1158. The authors appreciate the support of technical staff from Lamb Technicon, Warren, MI.

References

[1] Rivin EI, Kang H. Enhancement of dynamic stability of cantilever tooling structures. Int J Mach Tools Manuf 1992;32(4):539–61.

[2] Slocum AH, Marsh ER, Smith HD. A new damper design for machine tool structures: the replicated internal viscous dampler. Precis Eng 1994;16(3):174–83.

[3] Kim K, Eman KF, Wu SM. In-process control of cylindricity in boring operations. J Eng Indus 1987;109:291–6.
[4] Tewani, SG. Active optimal vibration control using dynamic absorber. In: IEEE International Conference on Robotics & Automation, Sacramento, CA, 1991.
[5] Browning DR, Golioto I, Thompson NB. Active Chatter Control System for Long-Overhang boring bars. In: SPIE Smart Structure and Material, San Diego, CA, 1997.
[6] Hanson DR, Tsao T. Development of a fast tool servo for variable-depth-of-cut machining. ASME Dynam Syst Contr 1994.
[7] Byrne G et al. Tool conditioning monitoring (TCM)—the status of research and industrial application. Ann CIRP 1995;44:541–67.
[8] Koren Y et al. Tool wear estimation under varying cutting conditions. Trans ASME—J Dyn Syst Contr 1991;113(2):300–7.
[9] Jemielniak K. Commercial Tool Condition Monitoring Systems. In: International Conference on Monitoring and Automatic Supervision in Manufacturing, AC'98, Warsaw, 1998.
[10] Franklin GF, Powell JD, Workman M. In: Digital control of dynamic systems. New York: Addison-Wesley; 1998, p. 310–337.
[11] Phillips CL, Nagle HT. In: Digital control system analysis and design. Englewood Cliffs, NJ: Prentice Hall; 1995, p. 413–420.
[12] Shiraishi M. Scope of in-process measurement, monitoring and control techniques in machining processes—Part 1: in-process techniques for tools. Precis Eng 1988:179–89.
[13] ANSI/ASME, Axes of Rotation. ASME Standard B89.3.4M, 1985, p. 30.